ELSEVIER

Journal of Nuclear Materials 294 (2001) 141–147

journal of nuclear materials

www.elsevier.nl/locate/jnucmat

The corrosion of Alloy 690 in high-temperature aqueous media – thermodynamic considerations

R.J. Lemire *, G.A. McRae

AECL, Chalk River Laboratories, Chalk River, Ont., Canada K0J 1J0

Abstract

Alloy 690 (N06690) is a technologically important material that contains a minimum of 58 wt% nickel, 27.0–31.0 wt% chromium and 7.0–11.0 wt% iron. A thermodynamic analysis of the expected behaviour of Alloy 690 in high-temperature (573 K) aqueous media has been carried out. The stabilization or destabilization of chromium, iron and nickel in the alloy has been taken into account using a variation of regular solution theory. Formation of polymetallic corrosion products, such as spinels, has also been considered. Reaction path calculations were performed for Alloy 690 at 573 K. The results are similar to those found from comparable calculations for the more widely used Alloy 600. Comparisons are made with available experimental observations.

1. Introduction

Alloy 690 (Inconel-690, N06690) is a technologically important material which contains a minimum of 58 wt% nickel, 27.0–31.0 wt% chromium and 7.0–11.0 wt% iron (Ni 55–64 at.%; Cr 29–34 at.%; Fe 7–11 at.%), with maximum limits of 0.5% for copper, manganese and silicon, 0.05 wt% for carbon and 0.015 wt% for sulfur. It has recently been put to use as a steam generator tube material in water-cooled nuclear power reactors as an alternative to Alloy 600 (Inconel-600) [1]. A typical steam generator at a nuclear electric power station contains several thousand thin-walled tubes operating in water at temperatures near 570 K. Steam generators are the main boundary between the pressurized, radioactive, primary cooling system and the lower-pressure secondary steam/condensate system. Significant corrosion of steam generator tubing has occurred at nuclear stations world-wide. In some cases this has required expensive replacement of complete units. Most of the failures have occurred with Alloy 600, and have been caused by various forms of environmental degradation including pitting, stress corrosion cracking and intergranular attack [2]. The performance of tubes made of Alloy 800 has been better. If a defective steam generator tube at a nuclear electric power station requires the unit to be shut down for repairs, the cost (primarily the cost of the reactor being unavailable) can be high. Replacing a complete steam generator can costs tens of millions of dollars. Thus, there are considerable economic and safety incentives to improve the corrosion performance of steam generators at water-cooled nuclear power reactors, by using Alloy 690 rather than Alloy 600.

Extensive research has been performed by the nuclear industry to better understand corrosion processes in steam generators and develop preventive measures. A comprehensive study of corrosion requires, as part of an interdisciplinary approach, a thermodynamic analysis of the system under consideration. Thermodynamic calculations can indicate whether or not chemical and electrochemical reactions causing corrosion are possible for various environments. Various authors have performed such calculations in the past, mainly in the form of potential-pH diagrams, for the nickel/water, iron/water, chromium/water and chromium/iron/water systems [3–6]. Few of these past analyses have considered the formation of polymetallic corrosion products or the effects of alloying.

* Corresponding author. Tel.: +1-613 584 3311; fax: +1-613 584 4220.

E-mail address: lemirer@aecl.ca (R.J. Lemire).

0022-3115/01/$ - see front matter
PII: S0022-3115(01)00468-8

Calculations of the thermodynamic behaviour of several alloys are being done at AECL. In this paper a thermodynamic analysis is done of the behaviour of Alloy 690 in high-temperature (573 K (300°C)) aqueous media. The stabilization or destabilization of nickel, iron and chromium in the alloys has been taken into account using a variation of regular solution theory. The formation of polymetallic corrosion products, such as spinels, has also been considered.

2. Thermodynamics of formation of Alloy 690

For the purposes of the present study, a single, simple composition of 60.5% Ni, 30.0% Cr and 9.5% Fe (at.%) has been assumed. The dissolution of an alloy in contact with an aqueous phase can be studied using thermodynamic calculations. The thermodynamic behaviour of the alloy will depend on the Gibbs energy of formation of the alloy. In turn, the Gibbs energy of formation is related to the activity coefficient of the constituent elements in the alloy. Thus, activity coefficient data are required for accurate thermodynamic calculations.

Dissolution of alloys takes place through oxidation processes. There is ample experimental evidence that the constituting elements of iron–nickel–chromium alloys retain their individual characteristics toward oxidation. For example, the cyclic voltammogram for type 316 L stainless steel is a composite of the voltammograms of its constituting elements [7]. Double layer capacity-potential curves, charge transfer resistance-potential curves and current–potential curves for type 304 L stainless steel show features typical of iron, nickel and chromium [8]. Iron and nickel are known to dissolve selectively from stainless steels during anodic polarization [9]. Indeed, it is now a widely held view that in low temperature aqueous solutions, passive films grow on stainless steels by the selective dissolution of components of the steel (see [10] and references therein). Iron–nickel–chromium alloy surfaces such as those of Alloy 690 can thus be assumed to oxidize (without oxidation of the bulk alloy), and then dissolve incongruently.

Alloy 690 is a fully austenitic alloy (probably only metastable at the temperatures below 600 K discussed here [11]). It is a single-phase solid solution of iron, nickel and chromium with a face-centred cubic crystalline structure (γ-phase) over a wide temperature range [12]. Thermodynamic data for three-component alloys are not usually available and must be calculated using various approximations. One such approximation is based on the formalism of regular solution theory. Alloying can be considered a mixing process where the stabilization or destabilization of the alloyed elements relative to their pure metallic states is due to the enthalpy and entropy of mixing. Regular solution theory assumes that the entropy of mixing of a regular solution is the same as for an ideal solution and is given by

$$\Delta_{\mathrm{m}}S = -R\sum_i x_i \ln x_i, \tag{1}$$

where $\Delta_{\mathrm{m}}S$ is the entropy of mixing, R is the gas constant and x_i is the atom fraction of component i. Thus, for regular solutions, only the enthalpy of mixing needs to be calculated. Hertzman and Sundman [11,13] have presented a thermodynamic model of the Fe–Ni–Cr system. Their model is based on a modification of regular solution theory and uses binary interaction coefficients to describe the enthalpy of mixing. Although this model is based on measured high-temperature (>1100 K) thermodynamic data, we assume the model can also be applied for lower temperatures.

According to their model, the standard Gibbs energy of formation of austenitic Fe–Ni–Cr solid solutions is given by

$$\Delta_{\mathrm{f}}G^{\circ}_{\mathrm{T}}(\mathrm{alloy}) = \sum_{i=1}^{3} x_i \Delta_{\mathrm{f}}G^{\circ}_{\mathrm{T}}(i,\mathrm{fcc}) + RT\sum_{i=1}^{3} x_i \ln x_i + {}^{E}G^{\circ}_{\mathrm{T}} + {}^{\mathrm{mag}}G^{\circ}_{\mathrm{T}}, \tag{2}$$

where $\Delta_{\mathrm{f}}G(\mathrm{alloy})$ is the standard Gibbs energy of formation of the alloy, $\Delta_{\mathrm{f}}G(i,\mathrm{fcc})$ is the standard Gibbs energy of formation of component i in the face-centred cubic structure of the alloy, T is the temperature in K, ${}^{\mathrm{E}}G$ is the excess Gibbs energy and ${}^{\mathrm{mag}}G$ is the contribution to the standard Gibbs energy due to magnetic ordering. The latter can be significant below the Curie temperature of the alloy. According to Hertzman and Sundman's model [11,13], the excess Gibbs energy is given by

$${}^{\mathrm{E}}G^{\circ}_{\mathrm{T}} = \sum_{i=1}^{2}\sum_{j>i}^{3}\sum_{b=0}^{3} x_i x_j (x_i - x_j)^b \cdot {}^{b}L_{i,j}, \tag{3}$$

where ${}^{b}L_{ij}$ are temperature-dependent binary interaction parameters. The contribution to the standard Gibbs energy due to magnetic ordering is given by

$$\begin{aligned} &{}^{\mathrm{mag}}G^{\circ}_{\mathrm{T}} = RT\ln(\beta+1)f(\tau,p)\\ &\tau = T/T_{\mathrm{c}}, \quad p = 0.28, \end{aligned} \tag{4}$$

where τ is T/T_{c}, T_{c} is the critical temperature for magnetic ordering in K and β is the average magnetic moment per atom for the alloy, in Bohr magneton [13]. The function $f(\tau,p)$ is

$$\begin{aligned} f(\tau,p) &= 1 - [79\tau^{-1}/140p + 474/497(1/p-1)\\ &\quad\times(\tau^3/6 + \tau^9/135 + \tau^{15}/600)]/A\\ &(\text{if } \tau \leqslant 1) \end{aligned} \tag{5}$$

$$\begin{aligned} f(\tau) &= -\{\tau^{-5}/10 + \tau^{-15}/315 + \tau^{-25}/1500\}/A\\ &(\text{if } \tau > 1), \end{aligned} \tag{6}$$

where

$$A = 518/1125 + 11692/15975(1/p - 1) \quad (7)$$

and the value of p depends on the structure of the alloy. According to Hertzman and Sundman [13], p has a value of 0.28 for face-centred cubic alloys. The composition dependence of T_c and β are given by equations similar in form to Eq. (3),

$$T_c = \sum_1^3 x_i T_c(i) + \sum_{i=1}^{2}\sum_{j>i}^{3}\sum_{b=0}^{3} x_i x_j (x_i - x_j)^b \cdot {}^bT_{i,j} + x_1 x_2 x_3 T_{1,2,3}, \quad (8)$$

$$\beta = \sum_1^3 x_i \beta(i) + \sum_{i=1}^{2}\sum_{j>i}^{3}\sum_{b=0}^{3} x_i x_j (x_i - x_j)^b \cdot {}^bB_{i,j} + x_1 x_2 x_3 B_{1,2,3}, \quad (9)$$

where $T_c(i)$ and $\beta(i)$ are the critical temperature for magnetic ordering and the average magnetic moment per atom for the pure components, respectively, ${}^bT_{i,j}$ and ${}^bB_{i,j}$ are temperature-dependent binary interaction parameters and $T_{1,2,3}$ and $B_{1,2,3}$ are the only ternary interaction terms required [14].

Using the parameters given by Chin et al. [14], Eq. (8) yields −370 K as the critical temperature for magnetic ordering for Alloy 690, and this corresponds to a Néel temperature of 123 K. The activity of component i in ternary solid solutions, a_i, can be calculated from the following expressions:

$$\mu_i(\text{alloy}) = \Delta_f G(i, \text{fcc}) + RT \ln a_i, \quad (10)$$

$$\mu_1(\text{alloy}) = \Delta_f G(\text{alloy}) - x_2\{\partial[\Delta_f G(\text{alloy})]/\partial x_2\} - x_3\{\partial[\Delta_f G(\text{alloy})]/\partial x_3\}, \quad (11)$$

$$\mu_2(\text{alloy}) = \Delta_f G(\text{alloy}) + (1 - x_2)\{\partial[\Delta_f G(\text{alloy})]/\partial x_2\} - x_3\{\partial[\Delta_f G(\text{alloy})]/\partial x_3\}, \quad (12)$$

$$\mu_3(\text{alloy}) = \Delta_f G(\text{alloy}) - x_2\{\partial[\Delta_f G(\text{alloy})]/\partial x_2\} + (1 - x_3)\{\partial[\Delta_f G(\text{alloy})]/\partial x_3\}, \quad (13)$$

where μ_i (alloy) is the chemical potential of component i in the alloy, and the partial derivatives are calculated using

$$x_1 = 1 - x_2 - x_3 \quad (14)$$

in the expression for $\Delta_f G$(alloy) (Eq. (2)). The standard Gibbs energy of formation of iron in the face-centred cubic structure of the alloys, $\Delta_f G$ (Fe, fcc), is assumed to be the same as that of γ-Fe, which has an identical crystal structure for temperatures above 900 K. The values given by Ågren [15] for ($\Delta_f G$ (Fe, fcc) $-\Delta_f G$ (Fe, bcc)) were used for lower temperatures, where the stable phase of iron is the body-centred cubic crystal structure (α-phase). The standard Gibbs energies of formation of chromium in the face-centred cubic structure as a function of temperature are available from the estimate of Kaufman and Nesor [16]. Elemental nickel has a face-centred cubic structure at temperatures up to its melting point. Its standard Gibbs energy of formation in the face-centred cubic structure of the alloys can thus be assumed to be the same as that of the element. Table 1 shows the activities of Fe, Ni and Cr in Alloy 690 at 298.15 and 573.15 K, as calculated from Eqs. (10)–(13). With respect to the pure metals, iron and nickel are strongly stabilized. Chromium is strongly destabilized. The activity values reported in Table 1 were used for all of the thermodynamic calculations described below.

Table 1
Calculated activities of Fe, Ni and Cr in Alloy 690 with respect to the standard states of the elements at the specified temperature

Component	Atom fraction	Activity	
		298 K	573 K
Fe	0.095	0.0097	0.027
Ni	0.605	0.091	0.282
Cr	0.300	156.7	5.063

3. Thermodynamic data

3.1. Data for metals in Alloy 690

The standard state for nickel at 298.15 K refers to the fcc-structure, while for iron and chromium the standard states refer to the bcc-phases. Although the bcc-phases are stable for both iron and chromium from 298 to 573 K, the calculations below were performed using values for the fcc-phases of iron, nickel and chromium (i.e., the phases consistent with the structures in the alloys). The Gibbs energies for the fcc forms for the three metals are given in Table 2, as are the values of the Gibbs energies for Fe, Ni and Cr in Alloy 690 with respect to the pure metals in their standard states at 298.15 K (i.e., the fcc-phase of Ni and the bcc-phases of Cr and Fe).

Table 2
Gibbs energies of formation for metals in Alloy 690 with respect to the metals in their standard states at 298.15 K

Metal	$\Delta_f G^\circ_{298}$ (kJ mol^{-1}) (pure fcc)	$\Delta_f G^\circ_{298}$ (kJ mol^{-1}) (in Alloy 690)	$\Delta_f G^\circ_{298}$ (kJ mol^{-1}) (in Alloy 690)
Cr	10.65	12.52	−1.34
Ni	0.0	−4.94	−16.84
Fe	5.4	−6.08	−24.38

3.2. Other chemical thermodynamic data

The full chemical thermodynamic database, aside from the values for the metals in the alloy (Table 2), will be reported elsewhere. Most of the chemical thermodynamic quantities for 298.15 K are from standard sources [17–21] or a previously published report [22]. Most high-temperature Gibbs energy values are estimated using literature heat capacity functions and extrapolation procedures discussed elsewhere [22–24]. Values for the transition metal hydrolysis species in basic solutions are based primarily on the work of Tremaine and LeBlanc [25,26] for iron and nickel and of Ziemniak et al. [27] and Hovey and Hepler [28] for chromium. Values for the mixed oxide phases are also from standard sources [17,19–21], though the value of $\Delta_f G^\circ$ adopted for $NiCr_2O_4$ (from [17]) likely overestimates the stability of that compound [29].

Values for γ-CrOOH(cr) and $Cr(OH)_3 \cdot 3H_2O$ are from Ziemniak et al. [27]. However, in assembling the database, we realized that if the thermodynamic quantities proposed by Ziemniak et al. [27] for γ-CrOOH(cr) are used with those for Cr_2O_3 (cr) [17,18,27] and H_2O(g), it should be possible to calculate the temperature at which the chromium hydroxide is dehydrated at a specified partial pressure of H_2O(g).

$$2\gamma\text{-CrOOH(cr)} = Cr_2O_3\text{(cr)} + H_2O\text{(g)} \qquad (15)$$

In fact, the calculation leads to a positive Gibbs energy of reaction even for temperatures well above that required for conversion of the solids in contact with fluid water [30]. Thus, the thermodynamic quantities of Ziemniak et al. [27] for γ-CrOOH(cr) should probably not be used for calculations for systems that do not include liquid water. We have not adjusted the thermodynamic quantities for γ-CrOOH for our present calculations. However, comparison with values for the corresponding aluminium solids suggests the estimated [27] value of S° (γ-CrOOH(cr)) is probably too large. Conversion of CrOOH(cr) to Cr_2O_3 (cr) (or more oxygen rich solids) is likely to occur at a temperature not much greater than 600 K for $P(H_2O) = 1$ bar, but only at considerably higher temperatures in contact with water at higher pressures [30].

4. Calculations

Potential-pH diagrams for iron, nickel and chromium in Alloy 690 (Figs. 1–3) were calculated using the computer program POTPH [31] for 298.15 and 573.15 K. The calculations allowed for formation of various stoichiometric mixed oxides, but not for their solid solution behaviour. In the diagrams, the aqueous solution species boundaries are those for dissolved species activities of 10^{-6} m. Reaction-path calculations were performed to describe the oxidative dissolution (corrosion) of Alloy 690. These were performed using the computer code CHEMP described by Garisto and Garisto [32], which is a modification of the Gibbs energy minimization code of Smith and Missen [33].

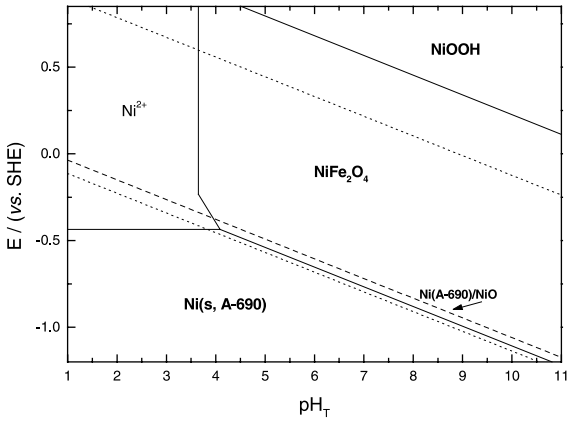

Fig. 1. Potential-pH diagram showing nickel solution species for the Alloy 690 Cr/Ni/Fe system at 573 K. The dotted lines represent the stability limits for water. The solid/dissolved species boundaries correspond to a dissolved species activity of 10^{-6} mol kg^{-1}. The dashed line shows the potential at which Ni (A-690) would be in equilibrium with NiO if $NiFe_2O_4$ did not form.

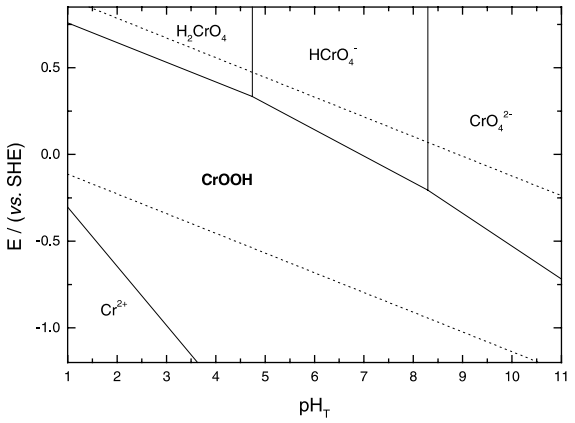

Fig. 2. Potential-pH diagram showing chromium solution species for the Alloy 690 Cr/Ni/Fe system at 573 K. The dotted lines represent the stability limits for water. The solid/dissolved species boundaries correspond to a dissolved species activity of 10^{-6} mol kg^{-1}.

5. Discussion

For near-neutral and mildly basic conditions, chromium metal is readily oxidized. Iron, and especially

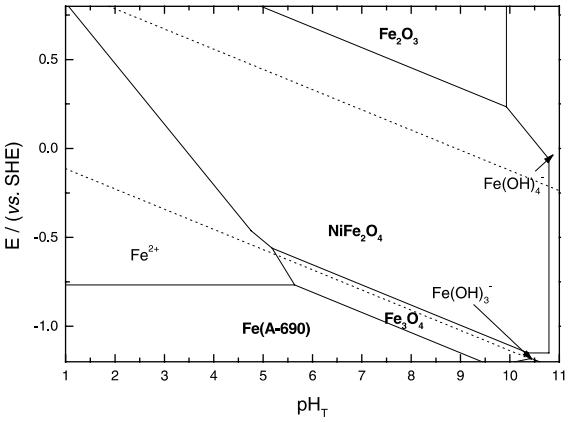

Fig. 3. Potential-pH diagram showing iron solution species for the Alloy 690 Cr/Ni/Fe system at 573 K. The dotted lines represent the stability limits for water. The solid/dissolved species boundaries correspond to a dissolved species activity of 10^{-6} mol kg^{-1}.

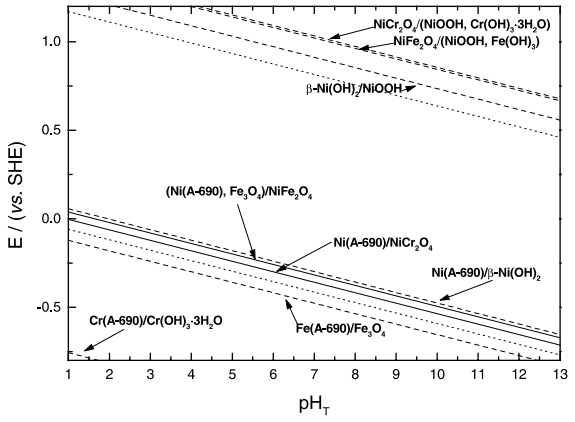

Fig. 4. A potential-pH diagram showing the equilibrium solids from aqueous oxidation of Alloy 690 at 298 K. No solution species are shown, but dotted lines representing the stability limits for water are shown for comparison.

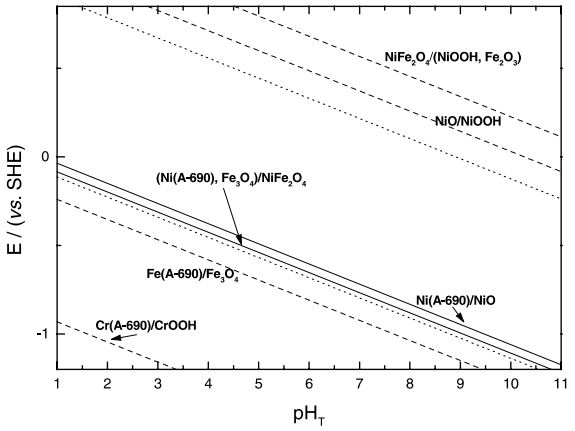

Fig. 5. A potential-pH diagram showing the equilibrium solids from hydrothermal oxidation of Alloy 690 at 573 K. No solution species are shown, but dotted lines representing the stability limits for water are shown for comparison.

nickel, are more resistant to oxidation. Figs. 1–3 show that for mildly basic oxidizing conditions (pH_T8–10) the equilibrium solution concentrations of chromium species are greater than those for nickel or iron. Thus, preferential leaching of chromium could occur at 573 K. Such behaviour might be expected for a wide pH range for oxidizing conditions, due to the stability of the chromate and protonated chromate ions. The surface of the alloys would then be covered by nickel and iron oxides ($NiO + Fe_2O_3$ or $NiFe_2O_4$). Conversely, for reducing conditions, the chromium solids are less susceptible to dissolution than those of iron or nickel. No evidence of preferential leaching of chromium from stainless steel components is found in nuclear reactor coolant, in which the concentration of chromium is much lower than 10^{-6} mol dm^{-3} (reducing conditions, 573 K – see, for example, [6]).

The stable solid phases that would be produced by progressive homogeneous oxidation of Alloy 690 are shown superimposed on the potential-pH diagrams in Figs. 4 and 5. The stability field of water is the region between the two dotted lines. Again, nickel ferrite is shown to have fairly large ranges of stability in water at 573 K.

Reaction path calculations were performed for fixed pH values of 10 at 298 K and 7, 8 and 9 at 573 K. These pH values at 573 K correspond approximately to solutions having the same aqueous hydroxide ion concentrations as room temperature solutions with pH values of 9.6, 10.6 and 11.6, respectively. For 298 K, at a pH value of 10, there are three potentials within the stability field of water at which four solids can coexist (in accordance with the phase rule) in equilibrium with aqueous solution. The sets of solids are (a) Ni(Alloy 690)/Fe_3O_4/$NiCr_2O_4$/$Cr(OH)_3 \cdot 3H_2O$, (b) Ni(Alloy 690)/Fe_3O_4/$NiCr_2O_4$/$NiFe_2O_4$ and (c) Ni(Alloy 690)/β-$Ni(OH)_2$/$NiCr_2O_4$/$NiFe_2O_4$. In the sequential oxidation of Alloy 690 at 573 K and for pH values between 7 and 9, there are two potentials within the stability field of water at which four solids can coexist – (d) Ni(Alloy 690)/Fe_3O_4/γ-CrOOH/$NiFe_2O_4$ and (e) Ni(Alloy 690)/NiO/γ-CrOOH/$NiFe_2O_4$. If any of these sets of solids is present on the alloy surface, the equilibrium concentrations of the solution species (and therefore the total equilibrium concentration of the metal in the water) are fixed. At constant temperature, these concentrations will remain constant until enough oxygen or hydrogen has been added to completely oxidize or reduce one of the

Table 3
Equilibrium aqueous concentrations for solutions buffered by sets of iron–nickel–chromium solids derived from Alloy 690

Alloy 690 solid set	$\log_{10}$ [Fe]	$\log_{10}$ [Cr]	$\log_{10}$ [Ni]	$\log_{10} p_{H_2(g)}$
298.15 K, $pH_T = 10$				
Ni(Alloy 690)/Fe_3O_4/$Cr(OH)_3 \cdot 3H_2O$	−8.5	−9.9	−11.1	>0.014
Ni(Alloy 690)/Fe_3O_4/$NiCr_2O_4$/$Cr(OH)_3 \cdot 3H_2O$	−8.5	−9.9	−11.1	0.014
Ni(Alloy 690)/Fe_3O_4/$NiCr_2O_4$/$NiFe_2O_4$	−8.9	−10.6	−9.7	0.00052
Ni(Alloy 690)/β-$Ni(OH)_2$/$NiCr_2O_4$/$NiFe_2O_4$	−9.6	−10.9	−9.0	0.00012
β-$Ni(OH)_2$/$NiCr_2O_4$/$NiFe_2O_4$	−9.6	−10.9	−9.0	<0.00012
573.15*K*, $pH_T = 7$				
Ni(Alloy 690)/Fe_3O_4/γ-CrOOH	−7.7	−10.2	−9.3	>0.31
Ni(Alloy 690)/Fe_3O_4/$NiFe_2O_4$/γ-CrOOH	−7.7	−10.2	−9.3	0.31
Ni(Alloy 690)/NiO/ $NiFe_2O_4$/γ-CrOOH	−8.3	−10.2	−8.5	0.044
NiO/$NiFe_2O_4$/γ-CrOOH	−8.3	−10.2	−8.5	<0.044
$pH_T = 8$				
Ni(Alloy 690)/Fe_3O_4/γ-CrOOH	−7.6	−10.0	−9.3	>0.31
Ni(Alloy 690)/Fe_3O_4/$NiFe_2O_4$/γ-CrOOH	−7.6	−10.0	−9.3	0.31
Ni(Alloy 690)/NiO/$NiFe_2O_4$/γ-CrOOH	−8.2	−10.0	−8.5	0.044
NiO/$NiFe_2O_4$/γ-CrOOH	−8.2	−10.0	−8.5	<0.044
$pH_T = 9$				
Ni(Alloy 690)/Fe_3O_4/γ-CrOOH	−7.1	−9.5	−9.0	>0.31
Ni(Alloy 690)/Fe_3O_4/$NiFe_2O_4$/γ-CrOOH	−7.1	−9.5	−9.0	0.31
Ni(Alloy 690)/NiO/$NiFe_2O_4$/γ-CrOOH	−7.6	−9.5	−8.2	0.044
NiO/$NiFe_2O_4$/γ-CrOOH	−7.6	−9.5	−8.2	<0.044

four solids on the surface. In effect, the solution concentrations are buffered by the set of solids. Because of the high nickel content of Alloy 690, elemental nickel and/or nickel oxide or hydroxide are dominant during the oxidation, and substantial buffering should occur only for sets (c) or (e). The solution concentrations of nickel-, iron- and chromium-containing solution species at the buffered potentials for pH values of 10 at 298.15 K and 7, 8 and 9 at 573.15 K are listed in Table 3.

As discussed above, it is probable that dehydration in air of γ-CrOOH at temperatures well above 298.15 K would result in formation of Cr_2O_3(cr) or the oxyhydroxide could be oxidized to form more oxygen-rich anhydrous chromium oxides. However, reaction path calculations suggest that air-oxidation of an Alloy 690 surface in the absence of water would, at equilibrium, result in formation of $NiCr_2O_4$, rather than Cr_2O_3(cr).

Several generalizations may be made from the calculated values reported in Table 3. The total solution concentration of iron species is generally greater than the total concentration of nickel or chromium species. Therefore, if metal is leached from the surface, the residual material should be depleted in iron. For reducing conditions within the stability field of water, the total solution concentrations of chromium species is less than the total solution concentrations of iron or nickel species, and this may generate a chromium-rich surface layer. A two-layer oxide is often observed on austenitic stainless steels exposed to high-temperature alkaline water [34]; a chromium-rich inner layer and an outer layer containing iron-rich spinels of the type $NiFe_2O_4$. However, under strongly oxidizing conditions chromium is substantially more soluble than iron or nickel. Therefore, phases precipitated under oxidizing conditions are likely to contain little chromium. The final products of oxidation are NiO, a small amount of $NiFe_2O_4$, and dissolved chromium species.

6. Conclusions

The reaction path calculations done in the present work cannot provide direct information on the mechanisms and kinetics of reaction at alloy surfaces. For example, thermodynamic arguments cannot be used to determine whether oxidized solids are formed from alloys by dissolution and precipitation, or by solid state transformation. The results of the thermodynamic calculations can be used, however, to rule out some mechanisms, and to provide some guidelines to the equilibrium behaviour at the Alloy 690 surface.

- Ni and Fe are stabilized in Alloy 690 relative to the pure metals; Cr is destabilized.
- Neither $NiCr_2O_4$ nor $FeCr_2O_4$ is expected to form as a stable surface phase at 573 K. It is possible $NiCr_2O_4$ might be an equilibrium solid phase at lower temperatures.
- At 573 K, in contact with basic reducing aqueous solutions, Ni, Fe_3O_4, and NiO are more soluble than γ-CrOOH.

- Thus, γ-CrOOH is expected to form as a surface film on Alloy 690 under those conditions.
- Under more oxidizing conditions γ-CrOOH can be oxidized to aqueous Cr(VI) species, and the stable surface phases would be expected to be a mixture of NiO and $NiFe_2O_4$ after leaching of the chromium from the alloy.
- $NiFe_2O_4$ is more stable than a mixture of an iron oxide or hydroxide (Fe_3O_4, Fe_2O_3 or $Fe(OH)_3$) with NiO or β-$Ni(OH)_2$ (except under extremely oxidizing conditions where nickel can be oxidized to NiOOH).
- If γ-CrOOH on a surface is heated in contact with water at temperatures above 560 K, conversion to other forms of CrOOH will occur [27], but the dehydration behaviour of these solids in air is not well established.
- Based on comparisons with values for other solids, the entropy of γ-CrOOH is probably considerably smaller than the value estimated by Ziemniak et al. [27]; thus, conversion of CrOOH to Cr_2O_3 is likely at a temperature not much greater than 600 K for $P(H_2O) = 1$ bar, but only at a considerably higher temperature in contact with water at higher pressures.
- Oxidation of the alloy surface in the absence of water could result in the formation of $NiCr_2O_4$ rather than Cr_2O_3.

Acknowledgements

The authors wish to express their appreciation to J. Paquette and F. Garisto of AECL who participated in carrying out similar, but unpublished, calculations for other alloys.

References

[1] R. Klarner, F. Steinmoeller, J. Millman, W. Schneider, in: Proc. Third Int. Steam Generator and Heat Exchanger Conf., Toronto, Canada, 1998, p. 17.
[2] D. Gómez-Briceño, M.L. Castaño, M.S. García, Nucl. Eng. Des. 165 (1996) 161.
[3] P. Radhakrishnamurty, P. Adaikkalam, Corros. Sci. 22 (1982) 753.
[4] C.M. Chen, K. Aral, G.J. Theus, Computer-Calculated Potential pH Diagrams to 300°C, Electric Power Research Institute Report EPRI-NP-3137, 1983.
[5] P.L. Daniel, S.L. Harper, Use of Pourbaix Diagrams to Infer Local Pitting Conditions, Electric Power Research Institute Report EPRI-NP-4831, 1986.
[6] D. Cubicciotti, J. Nucl. Mater. 167 (1989) 241.
[7] N. Ramasubramanian, N. Preocanin, R.D. Davidson, J. Electrochem. Soc. 132 (1985) 703.
[8] J.A. Harisson, D.E. Williams, Electrochim. Acta 31 (1986) 1063.
[9] J.E. Castle, J.H. Qiu, J. Electrochem. Soc. 137 (1990) 2031.
[10] J. Robertson, Corros. Sci. 32 (1991) 443.
[11] S. Hertzman, B. Sundman, Scand. J. Metall. 14 (1985) 94.
[12] V.G. Rivlin, G.V. Raynor, Int. Metall. Rev. 1 (1980) 21.
[13] S. Hertzman, B. Sundman, CALPHAD 6 (1982) 67.
[14] C.-P. Chin, S. Hertzman, B. Sundman, An Evaluation of the Composition Dependence of the Magnetic Order-Disorder Transition in Cr–Fe–Co–Ni Alloys, Materials Research Center, The Royal Institute of Technology (Stockholm, Sweden), Report TRITA-MAC 203, 1987.
[15] J. Ågren, Metall. Trans. 10A (1979) 1847.
[16] L. Kaufman, H. Nesor, Z. Metallkd. 64 (1973) 249.
[17] G.B. Naumov, B.N. Ryzhenko, I.L. Khodakovsky, 1971., Handbook of Thermodynamic Data, Moscow: Atomizdat, Report WRD-74-01, U.S. Geological Survey, Menlo Park, CA, 1974 (G.J. Soleimani, I. Barnes, V. Spelz, Trans. from Russian).
[18] I. Dellien, F.M. Hall, L.G. Hepler, Chem. Rev. 76 (1976) 283.
[19] I. Barin, O. Knacke, Thermochemical Properties of Inorganic Substances, Springer, Berlin, 1973.
[20] I. Barin, O. Knacke, O. Kubaschewski, Thermochemical Properties of Inorganic Substances. Springer, Berlin, 1977 (Suppl.).
[21] D.D. Wagman, W.H. Evans, V.B. Parker, R.H. Schumm, I. Halow, S.M. Bailey, K.L. Churney, R.L. Nuttall, J. Phys. Chem. Ref. Data 11 (Suppl. 2) (1982).
[22] D.J. Jobe, R.J. Lemire, P. Taylor, Iron Oxide Redox Chemistry and Nuclear Fuel Disposal Atomic Energy of Canada Limited Report AECL-11667 (COG-96-487-I) 1997.
[23] C.M. Criss, J.W. Cobble, J. Am. Chem. Soc. 86 (1964) 5390.
[24] E.L. Shock, H.C. Helgeson, Geochim. Cosmochim. Acta 52 (1988) 2009; errata, ibid 53 (1989) 215.
[25] P.R. Tremaine, J.C. LeBlanc, J. Solution Chem. 9 (1980) 415.
[26] P.R. Tremaine, J.C. LeBlanc, J. Chem. Thermodyn. 12 (1980) 521.
[27] S.E. Ziemniak, M.E. Jones, K.E.S. Combs, J. Solution Chem. 27 (1998) 33.
[28] J.K. Hovey, L.G. Hepler, J. Phys. Chem. 94 (1990) 7821.
[29] E.B. Rudnyi, E.A. Kaibicheva, L.N. Sidorov, M.T. Varshavskii, A.N. Men, J. Chem. Thermodyn. 22 (1990) 623.
[30] M.W. Shafer, R. Roy, Z. Anorg. Allg. Chem. 276 (1954) 275.
[31] J. Paquette, R.J. Lemire, Nucl. Sci. Eng. 79 (1981) 26.
[32] N.C. Garisto, F. Garisto, Nucl. Chem. Waste Manag. 5 (1984) 17.
[33] W.R. Smith, R.W. Missen, Chemical Reaction Equilibrium Analysis: Theory and Algorithms, Wiley, New York, 1982.
[34] R.L. Tapping, R.D. Davidson, E. McAlpine, D.H. Lister, Corros. Sci. 26 (1986) 563.